

Multi-Spherical Diffusion MRI: An in-vivo Test- Retest Study of Time-Dependent q-space Indices

Rutger H.J. Fick, Alexandra Petiet, Mathieu Santin, Anne-Charlotte Philippe, Stéphane Lehéricy, Rachid Deriche, Demian Wassermann

▶ To cite this version:

Rutger H.J. Fick, Alexandra Petiet, Mathieu Santin, Anne-Charlotte Philippe, Stéphane Lehéricy, et al.. Multi-Spherical Diffusion MRI: An in-vivo Test- Retest Study of Time-Dependent q-space Indices. ISMRM: 25th Annual Meeting & Exhibition, Apr 2017, Honolulu, United States. hal-01468214

HAL Id: hal-01468214 https://hal.science/hal-01468214v1

Submitted on 23 Feb 2017

HAL is a multi-disciplinary open access archive for the deposit and dissemination of scientific research documents, whether they are published or not. The documents may come from teaching and research institutions in France or abroad, or from public or private research centers. L'archive ouverte pluridisciplinaire **HAL**, est destinée au dépôt et à la diffusion de documents scientifiques de niveau recherche, publiés ou non, émanant des établissements d'enseignement et de recherche français ou étrangers, des laboratoires publics ou privés.

Multi-Spherical Diffusion MRI: An in-vivo Test-Retest Study of Time-Dependent q-space Indices

Rutger Fick* Alexandra Petiet[†] Mathieu Santin[†] Anne-Charlotte Philippe[†] Stephane Lehericy[†] Rachid Deriche^{*} Demian Wassermann^{*} * Université Côte d'Azur, INRIA, France [†] CENIR, ICM, Paris, France

Contact - rutger361988@gmail.com / demian.wassermann@inria.fr

http://team.inria.fr/athena/

Abstract: We assess the test-retest reproducibility of time-dependent q-space indices ($q\tau$ -indices) in three C57BI6 wildtype mice. To estimate $q\tau$ -indices from the four-dimensional $q\tau$ diffusion signal - varying over 3D q-space and diffusion time - we use our recent Multi-Spherical Diffusion MRI (MS-dMRI) method. Using MS-dMRI we could reliably estimate $q\tau$ indices for two out of three subjects, where acquisition artifacts caused the offsets of the last subject.

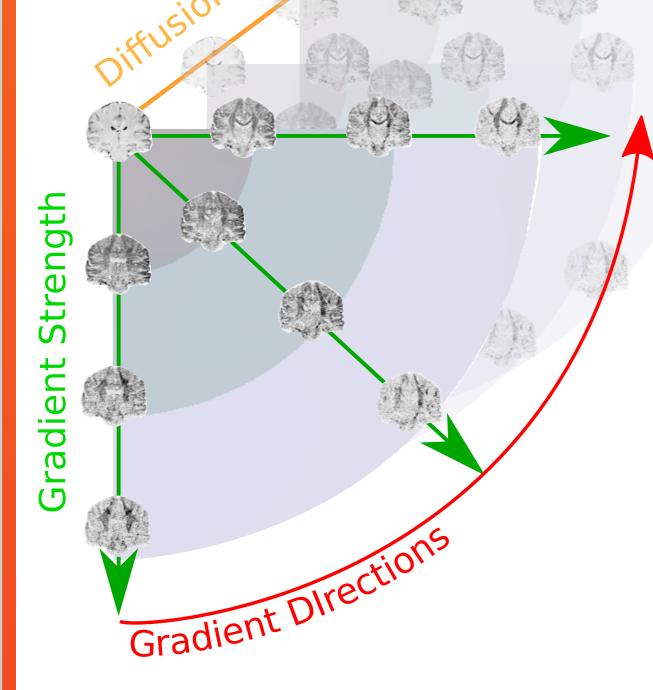
1 The 4D qτ-diffusion signal

Diffusion restriction occurs when

2 Modeling the qτ-signal using MS-dMRI

MS-dMRI uses a separable Fourier Basis to reconstruct



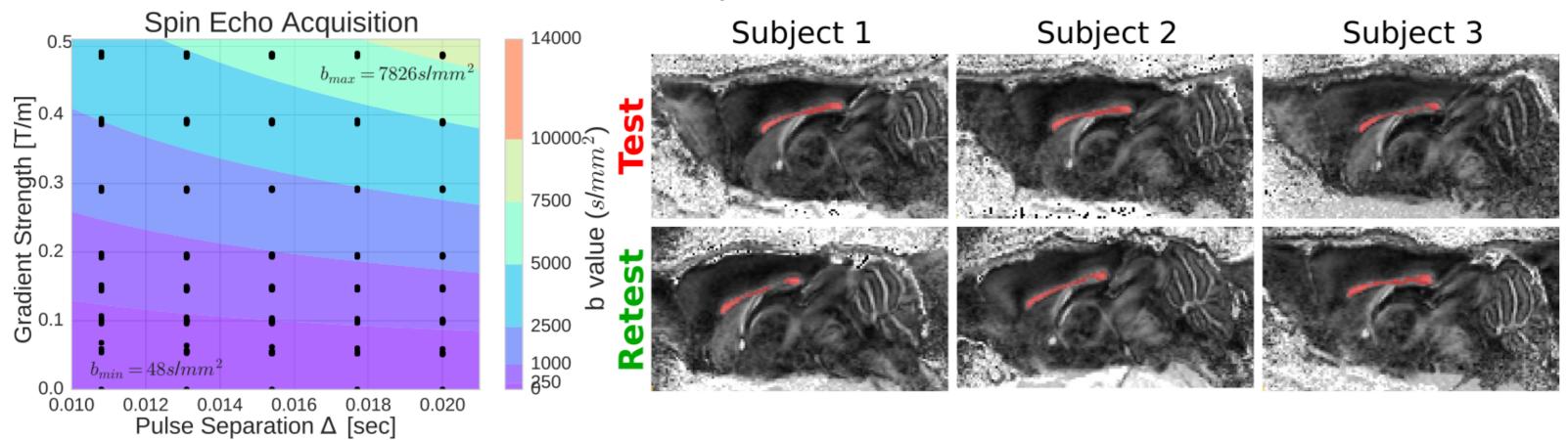


water diffusion is obstructed by tissue boundaries. The amount of restriction is **time-dependent**, meaning that the observed diffusion coefficient will change for varying diffusion times [1].

Multi-Spherical dMRI (MS-DMRI) [2] describes the qτ-diffusion signal [3] over varying:

- Gradient strength (G)
- Gradient direction (g)
- Diffusion time (τ)

Data Description: We acquire 3 test-retest mouse datasets (35 shells, 580 DWIs) with G_{max} =490mT/m and 10.8< τ <20ms.



diffusion propagator $P(\mathbf{r},\tau;\mathbf{c})$ from signal attenuation E $(\mathbf{q},\tau;\mathbf{c})$, represented in coefficients **c**.

 $\hat{E}(\mathbf{q},\tau;\mathbf{c}) = \sum_{i}^{N_{\mathbf{q}}} \sum_{k}^{N_{\tau}} \mathbf{c}_{ik} \Phi_{i}(\mathbf{q}) T_{k}(\tau) \quad \stackrel{\text{FT}}{\iff} \quad \hat{P}(\mathbf{r},\tau;\mathbf{c}) = \sum_{i}^{N_{\mathbf{q}}} \sum_{k}^{N_{\tau}} \mathbf{c}_{ik} \Psi_{i}(\mathbf{r}) T_{k}(\tau)$

 $\Psi_i(\mathbf{r}) = FT(\Phi_i(\mathbf{q}))$: 3D *Fourier* basis over **q** and displacement **r** [4]. $T_m(\tau)$: Exponential diffusion time basis over τ [5].

We constrain the fitting of **c** to respect boundary conditions of the signal and impose **signal smoothness and sparsity**:

$$\operatorname{argmin}_{\mathbf{c}} \underbrace{\int \int \left[E(\mathbf{q},\tau) - \hat{E}(\mathbf{q},\tau;\mathbf{c}) \right]^2 d\mathbf{q} d\tau}_{(2) \operatorname{Smoothness}} + \underbrace{\int \int \left[\nabla^2 \hat{E}(\mathbf{q},\tau;\mathbf{c}) \right]^2 d\mathbf{q} d\tau}_{(3) \operatorname{Sparsity}} + \underbrace{\int \int \left[\nabla^2 \hat{E}(\mathbf{q},\tau;\mathbf{c}) \right]^2 d\mathbf{q} d\tau}_{(2) \operatorname{Smoothness}} + \underbrace{\int \int \left[\nabla^2 \hat{E}(\mathbf{q},\tau;\mathbf{c}) \right]^2 d\mathbf{q} d\tau}_{(2) \operatorname{Smoothness}} + \underbrace{\int \int \left[\nabla^2 \hat{E}(\mathbf{q},\tau;\mathbf{c}) \right]^2 d\mathbf{q} d\tau}_{(2) \operatorname{Smoothness}} + \underbrace{\int \int \left[\nabla^2 \hat{E}(\mathbf{q},\tau;\mathbf{c}) \right]^2 d\mathbf{q} d\tau}_{(2) \operatorname{Smoothness}} + \underbrace{\int \int \left[\nabla^2 \hat{E}(\mathbf{q},\tau;\mathbf{c}) \right]^2 d\mathbf{q} d\tau}_{(2) \operatorname{Smoothness}} + \underbrace{\int \int \left[\nabla^2 \hat{E}(\mathbf{q},\tau;\mathbf{c}) \right]^2 d\mathbf{q} d\tau}_{(2) \operatorname{Smoothness}} + \underbrace{\int \int \left[\nabla^2 \hat{E}(\mathbf{q},\tau;\mathbf{c}) \right]^2 d\mathbf{q} d\tau}_{(2) \operatorname{Smoothness}} + \underbrace{\int \int \left[\nabla^2 \hat{E}(\mathbf{q},\tau;\mathbf{c}) \right]^2 d\mathbf{q} d\tau}_{(2) \operatorname{Smoothness}} + \underbrace{\int \int \left[\nabla^2 \hat{E}(\mathbf{q},\tau;\mathbf{c}) \right]^2 d\mathbf{q} d\tau}_{(2) \operatorname{Smoothness}} + \underbrace{\int \int \left[\nabla^2 \hat{E}(\mathbf{q},\tau;\mathbf{c}) \right]^2 d\mathbf{q} d\tau}_{(2) \operatorname{Smoothness}} + \underbrace{\int \int \left[\nabla^2 \hat{E}(\mathbf{q},\tau;\mathbf{c}) \right]^2 d\mathbf{q} d\tau}_{(2) \operatorname{Smoothness}} + \underbrace{\int \int \left[\nabla^2 \hat{E}(\mathbf{q},\tau;\mathbf{c}) \right]^2 d\mathbf{q} d\tau}_{(2) \operatorname{Smoothness}} + \underbrace{\int \int \left[\nabla^2 \hat{E}(\mathbf{q},\tau;\mathbf{c}) \right]^2 d\mathbf{q} d\tau}_{(2) \operatorname{Smoothness}} + \underbrace{\int \left[\nabla^2 \hat{E}(\mathbf{q},\tau;\mathbf{c}) \right]^2 d\mathbf{q} d\tau}_{(2) \operatorname{Smoothness}} + \underbrace{\int \left[\nabla^2 \hat{E}(\mathbf{q},\tau;\mathbf{c}) \right]^2 d\mathbf{q} d\tau}_{(2) \operatorname{Smoothness}} + \underbrace{\int \left[\nabla^2 \hat{E}(\mathbf{q},\tau;\mathbf{c}) \right]^2 d\mathbf{q} d\tau}_{(2) \operatorname{Smoothness}} + \underbrace{\int \left[\nabla^2 \hat{E}(\mathbf{q},\tau;\mathbf{c}) \right]^2 d\mathbf{q} d\tau}_{(2) \operatorname{Smoothness}} + \underbrace{\int \left[\nabla^2 \hat{E}(\mathbf{q},\tau;\mathbf{c}) \right]^2 d\mathbf{q} d\tau}_{(2) \operatorname{Smoothness}} + \underbrace{\int \left[\nabla^2 \hat{E}(\mathbf{q},\tau;\mathbf{c}) \right]^2 d\mathbf{q} d\tau}_{(2) \operatorname{Smoothness}} + \underbrace{\int \left[\nabla^2 \hat{E}(\mathbf{q},\tau;\mathbf{c}) \right]^2 d\mathbf{q} d\tau}_{(2) \operatorname{Smoothness}} + \underbrace{\int \left[\nabla^2 \hat{E}(\mathbf{q},\tau;\mathbf{c}) \right]^2 d\mathbf{q} d\tau}_{(2) \operatorname{Smoothness}} + \underbrace{\int \left[\nabla^2 \hat{E}(\mathbf{q},\tau;\mathbf{c}) \right]^2 d\mathbf{q} d\tau}_{(2) \operatorname{Smoothness}} + \underbrace{\int \left[\nabla^2 \hat{E}(\mathbf{q},\tau;\mathbf{c}) \right]^2 d\mathbf{q} d\tau}_{(2) \operatorname{Smoothness}} + \underbrace{\int \left[\nabla^2 \hat{E}(\mathbf{q},\tau;\mathbf{c}) \right]^2 d\mathbf{q} d\tau}_{(2) \operatorname{Smoothness}} + \underbrace{\int \left[\nabla^2 \hat{E}(\mathbf{q},\tau;\mathbf{c}) \right]^2 d\mathbf{q} d\tau}_{(2) \operatorname{Smoothness}} + \underbrace{\int \left[\nabla^2 \hat{E}(\mathbf{q},\tau;\mathbf{c}) \right]^2 d\mathbf{q} d\tau}_{(2) \operatorname{Smoothness}} + \underbrace{\int \left[\nabla^2 \hat{E}(\mathbf{q},\tau;\mathbf{c}) \right]^2 d\mathbf{q} d\tau}_{(2) \operatorname{Smoothness}} + \underbrace{\int \left[\nabla^2 \hat{E}(\mathbf{q},\tau;\mathbf{c}) \right]^2 d\mathbf{q} d\tau}_{(2) \operatorname{Smoothness}} + \underbrace{\int \left[\nabla^2$$

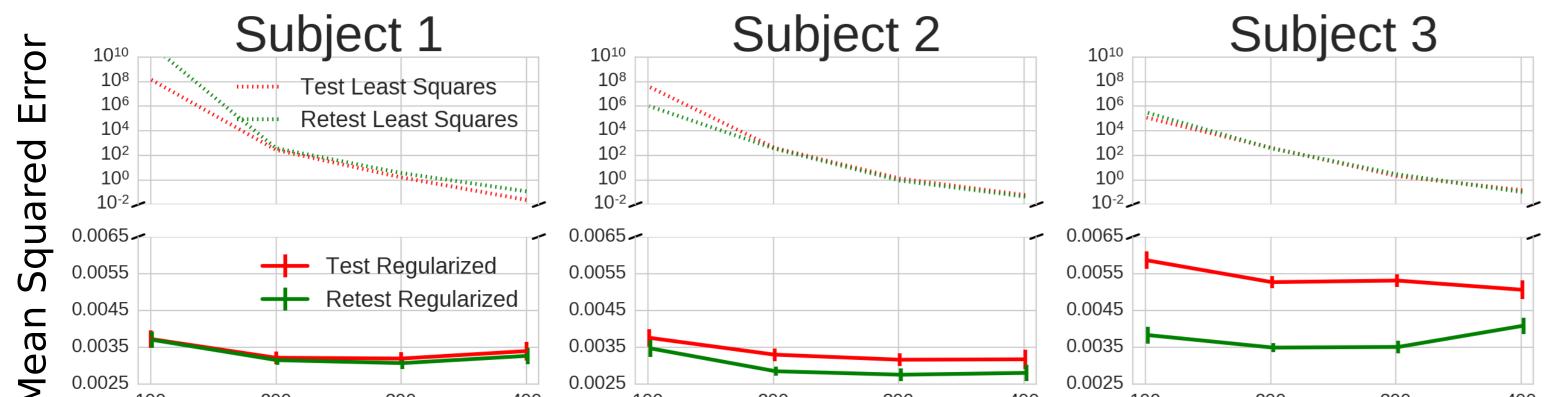
Once fitted, we can estimate, for any τ , the q-space indices Mean Squared Displacement (MSD) and Return-to-Origin, Axis and Plane Probability (RTOP, RTAP, RTPP) [4]:

MSD: related to restriction
RTOP: related to cellularity
RTOP: related to cellularity

3 Test-Retest of Subsampling Fitting Error

We draw an ROI in the **corpus callosum** in each data set. We estimate the fitting error using MS-dMRI when randomly subsampling the qt-signal down from 400 to 100 samples.

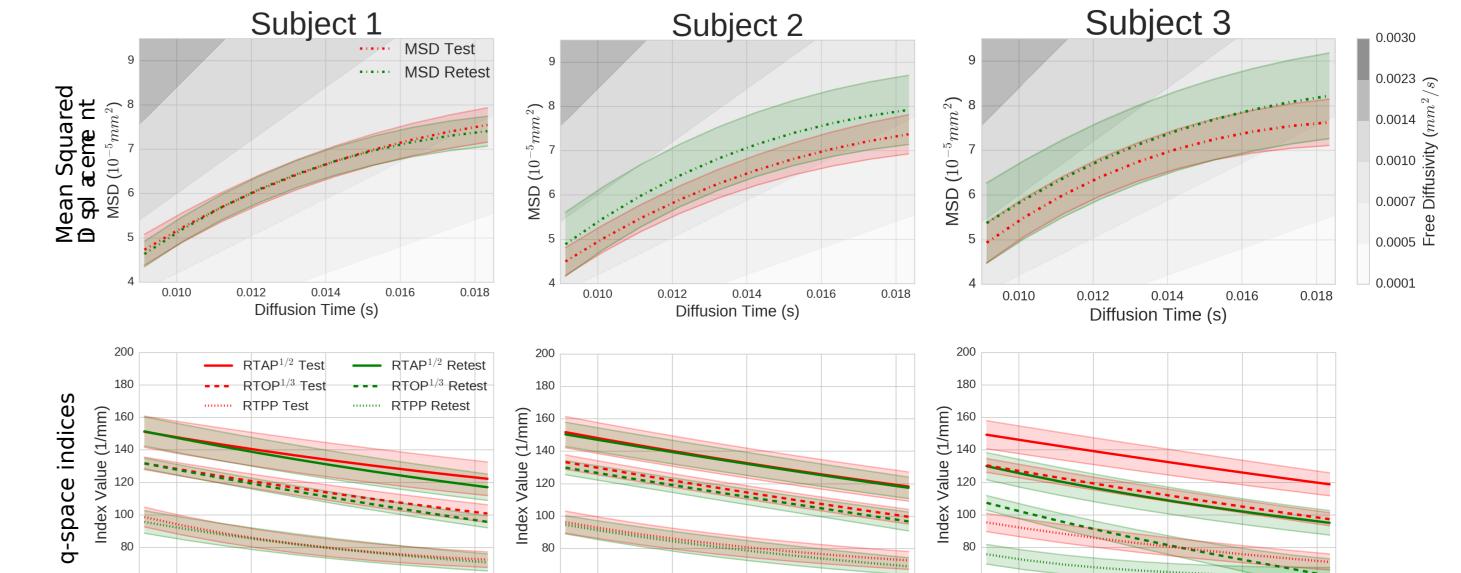
- Without regularization (dashed) the fitting error is up to 10 orders of magnitude larger than with regularization (solid).
- Only Subject 3 has inconsistent test-retest fitting errors.
- With regularization we find a **lower bound of 200 DWIs** while ensuring a low fitting error (solid lines).



4 Test-Retest of qτ-index Estimation

Using the whole data, we estimate the progress of the average MSD, RTOP, RTAP and RTPP and 0.75 standard deviation over time. The gray tones show MSD isolines for different free diffusion coefficients. Notice the non-Gaussian MSD progress.

- Subject 1: Great test-retest reproducibility all indices.
- Subject 2: Similar overlap for RTXP indices, small offset MSD.
- Subject 3: Offset for both RTXP indices and MSD.



 100
 200
 300
 400
 100
 200
 300
 400
 100
 200
 300
 400
 100
 200
 300
 400
 100
 200
 300
 400
 100
 200
 300
 400
 100
 200
 300
 400
 100
 200
 300
 400
 100
 200
 300
 400
 100
 200
 300
 400
 100
 200
 300
 400
 100
 200
 300
 400
 100
 200
 300
 400
 100
 200
 300
 400
 100
 200
 300
 400
 100
 200
 300
 400
 100
 200
 300
 400
 100
 200
 100
 200
 100
 200
 100
 200
 100
 200
 100
 200
 100
 200
 100
 200
 100
 200
 100
 200
 100
 200
 100
 200
 100
 200
 100
 200
 100
 200
 100
 200
 100
 200
 100
 200
 100
 200
 2

5 Discussion and Conclusions

- We studied the test-retest reproducibility of fitting error and $q\tau$ -index estimation in the corpus callosum of three mice.
- Through signal sparsity and smoothness, MS-dMRI can represent the qt-signal using only 200 samples, allowing more realistic acquisition schemes.
- The acquisition protocol can still be improved to avoid excessive acquisition noise like in Subject 3.
- Overall, we found that MS-dMRI can robustly and consistently estimate $q\tau$ -indices in in-vivo acquisitions, underlining its feasibility to estimate τ -dependent features.

ATHENA - INRIA - FRANCE

Acknowledgements: This work has received funding from the European Research Council (ERC) under the Horizon 2020 research and innovation program (ERC Advanced Grant agreement No 694665 : CoBCoM) and from the ANR-13-MONU-0009 MOSIFAH project.

References [1] Fieremans et al. NeuroImage 129 (2016): 414-427. [2] Fick et al. CD-MRI 2016. [3] Novikov et al. arXIV:1612.02059 (2016) [4] Özarslan et al. NeuroImage 78 (2013): 16-32. [5] Fick et al. IPMI 2015.

ISMRM: 25th Annual Meeting & Exhibition, 2017, 22 - 27 April, Honolulu - Hawaii